BIOCHEMISTRY
including biophysical chemistry & molecular biology

Article

pubs.acs.org/biochemistry

Spectroscopic Analysis of the Effect of Chloride on the Active Intermediates of the Primate L Group Cone Visual Pigment

Takefumi Morizumi,[†] Keita Sato, and Yoshinori Shichida*

Department of Biophysics, Graduate School of Science, Kyoto University, Kyoto 606-8502, Japan

ABSTRACT: Cone visual pigments responsible for color vision are classified into four groups; among these, the L(LWS) group contains the visual pigments having the most red-shifted λ_{max} and a chloride-binding site in their protein moiety. Binding of chloride results in the so-called "chloride effect", e.g., the red shift of λ_{max} and the faster decay of meta-I. These properties disappear upon replacement of chloride with nitrate. Because the amino acid residue primary responsible for the chloride effect is H197, we have replaced this residue with 19 other amino acids to gain insights into the mechanism creating these properties. Of the 19 single-site mutants, 13 were successfully expressed and bound 11-*cis*-retinal to form pigments. Eleven of the 13 mutants exhibited a red shift of λ_{max} upon chloride binding, and histidine produced the most red-shifted λ_{max}. We classified H197 mutants into three groups according to their properties. The first group of mutants exhibited a chloride effect similar to that of the wild type, while the second group of mutants showed no chloride effect. The third group of mutants exhibited a small shift in λ_{max} and enhanced decay rates of meta-I upon chloride binding. Furthermore, some of the mutants in this group showed meta-I decay faster than that of the wild type and extraordinarily fast decays of meta-I even in the absence of chloride. Interestingly, amino acid residues in the third group of mutants are characterized by their propensity to form β-sheets. These results suggest that the acquisition of H197 would be due to the most red-shifted absorption maximum, resulting in fast formation of the active state.

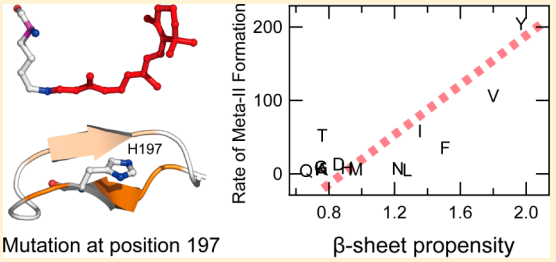

Visual transduction in vertebrate photoreceptor cells begins with the absorption of a photon by visual pigments, retinal-based photoreceptive proteins belonging to the group of G protein-coupled receptors.[1−3] Phylogenetic analysis shows that vertebrate visual pigments are classified into a rod visual pigment (Rh group) and four cone visual pigments [S (SWS1), M1 (SWS2), M2 (Rh2), and L (LWS) groups].[4] The presence of multiple cone visual pigments with different absorption maxima is the molecular basis of color discrimination. We have been investigating the molecular properties of visual pigments, as differences in their molecular properties such as photoreactions and thermal stabilities can potentially affect the photoresponses of photoreceptor cells having these pigments. We first compared rod and cone visual pigments and revealed that although photosensitivities of these pigments are not so different, the formation and decay rates of the G protein activating state meta-II are greatly different.[2,5,6] Furthermore, we conducted a comparative analysis of the photobleaching processes of the four kinds of cone visual pigments.[7] Detailed analyses of the photoreaction of these pigments showed that S, M1, and M2 group pigments exhibited a photobleaching process that was very similar to that of rhodopsin, in contrast with the L group cone visual pigment that exhibited a unique reaction process. Although the L group pigment formed a mixture of meta-I and meta-II similar to those of the other cone visual pigments and rhodopsin, these intermediates formed much faster. Moreover, the pH-dependent equilibrium between meta-I and meta-II, characteristic of rhodopsin, could not be observed in the L group, whereas the other cone pigments (S, M1, and M2) exhibited a reaction similar to that of rhodopsin. Finally, there was little indication of the formation of meta-III in the L group. Therefore, cone pigments in the L group have a reaction mechanism different from that of the other cone visual pigments and rhodopsin.

It is well-known that cone pigments in the L group have a chloride-binding site in their protein moiety,[8−10] which differentiates cone pigments in the L group from the other visual pigments. We have previously shown that the molecular properties characteristic of L group cone pigments can be eliminated by replacement of chloride with nitrate.[7] That is, the characteristic reactions observed in cone pigments in the L group can be attributed to the binding of chloride.

We used mfas green (*Macaca fascicularis* green cone visual pigment) as a representative member of the L group cone pigments. The amino acid residues responsible for chloride binding are H197 and K200, where H197 is the primary residue responsible for the chloride effect.[11] We replaced H197 in mfas green with the other 19 amino acids and investigated changes in the molecular properties of these single-site mutants. Pigments were successfully obtained from 13 of the 19 single-site mutants, and among the expressed mutants, 11 exhibited a red shift of the absorption maximum upon chloride binding. The mutant proteins could be categorized into three groups, based on their molecular properties. One group exhibited molecular

Received: July 24, 2012
Revised: November 1, 2012
Published: November 26, 2012

properties very similar to those of the wild type, although the extent of the chloride effect is somewhat weaker. The second group exhibited no chloride effect, suggesting that replacement of the amino acid residue caused the loss of chloride binding. The third group exhibited a small shift in absorption maxima but an enhanced rate of decay of meta-I; some members in this group showed meta-I decay that was faster than that of the wild type. Additionally, these mutants also showed fast decay of meta-I even in the nitrate-bound form. The mutants belonging to the third group contain amino acid residues with a strong propensity to form a β-sheet, according to Chou and Fasman.[12] These results suggest that formation of active meta-II is accompanied by the formation of β-sheet structure in the L group visual pigments, and one of the roles of chloride binding is to enhance β-sheet formation. On the basis of these results, we will discuss the physiological significance of chloride binding in the L group pigments.

MATERIALS AND METHODS

Preparation of the mfas Green WT and Its Mutants. The wild-type (WT) and mutant pigments of mfas green were expressed in HEK293 cells as previously reported.[13−15] For purification, the cDNAs of the pigments were tagged with the monoclonal antibody Rho1D4 epitope sequence (ETSQVA-PA).[15] The cDNAs of site-directed mutant pigments were constructed following the method used in a previous report.[16] The cDNAs of wild-type and mutant pigments were fully sequenced before being introduced into the expression vector.[17] To reconstitute photoreactive pigments, expressed proteins were incubated with 11-*cis*-retinal for more than 3 h at 4 °C. The reconstituted pigments were extracted in buffer A [0.75% (w/v) CHAPS, 0.8 mg/mL PC, 50 mM HEPES, 140 mM NaCl, and 2 mM $MgCl_2$ (pH 6.5)], and pigments were then purified with an antibody-conjugated column.[18] Pigments were washed and eluted with buffer A for the chloride-bound measurements or buffer B [0.75% (w/v) CHAPS, 0.8 mg/mL PC, 50 mM HEPES, 140 mM $NaNO_3$, and 2 mM $Mg(NO_3)_2$ (pH 6.5)] for the chloride-unbound measurements.

Spectroscopy. The UV−vis absorption spectra were recorded using two types of spectrophotometers. Absorption spectra of the dark and completely bleached states of the pigments were recorded with a Shimadzu UV-2400 spectrophotometer. The time-resolved absorbance changes were recorded by a CCD spectrophotometer described previously.[19] This spectrophotometer can continuously record the spectra (from 700 to 300 nm) with a wavelength resolution of 1.57 nm in time intervals of 9.7 ms. The monitoring light is pulsed after the first 1 s and hit the sample only when each spectrum was measured. Rhodopsin bleaching in the sample caused by monitoring light was ∼1.85% after 100 spectra recordings, which is comparable to that observed in a commercial spectrophotometer, such as a Shimadzu UV-2000 spectrophotometer. The sample temperature was regulated within 0.1 °C by a temperature controller (Neslab RTE-111) that was attached to the sample cell holder. The sample was incubated for 30 min at 4 °C and then photoexcited with a >520 nm light pulse (width of ∼170 μs, intensity of ∼0.7 mJ/1.8 mmϕ) from a short ark flash generator (Nissin Electronic SA-200). Excitation was performed 97 ms after the monitoring had started. The spectral changes caused by the thermal reactions of the intermediate were monitored at intervals of 9.7 ms to 1 s or at suitable intervals until the reactions had nearly reached saturation. The sample was exchanged after each measurement.

The relatively high expression yield of WT mfas green allowed us to monitor the thermal reactions of chloride- and nitrate-bound mfas greens from 9.7 ms to 1000 s, in which decay of meta-I to a mixture of meta-I and meta-II and the decay of the mixture were completed. However, in addition to the inevitable baseline drift of the spectrophotometer for prolonged monitoring, low expression yields of several mutants prevented us from monitoring the reactions for more than 100 s. Thus, it was very difficult to obtain a set of spectral data that included complete decay of the meta-I/meta-II mixture of the mutants. Therefore, we subjected the data of spectral changes obtained from 9.7 ms to 10 s to singular-value decomposition (SVD) and global fitting analyses to obtain the b-spectra and the decay time constant due to the reaction process from meta-I to a mixture of meta-I and meta-II (see below).

Data Analysis. The spectral changes of intermediates were analyzed by SVD and global fitting methods as previously described, using Igor Pro (WaveMetrics Inc.).[7,20] Briefly, the difference spectra were arranged in matrix **A** so that its columns and rows corresponded to wavelength and acquisition time. The SVD decomposed **A** into a product of a left singular matrix, **U**, a diagonal matrix containing singular values, **S**, and a transpose of a right singular matrix, **V**, as follows.

$$\mathbf{A} = \mathbf{U}\cdot\mathbf{S}\cdot\mathbf{V}^T \quad (1)$$

The number of columns considered for the following estimation was determined on the basis of the number of significant singular values and basis spectra in matrices **U** and **V**.

$$\mathbf{U}\cdot\mathbf{S}\cdot\mathbf{V}^T \approx \mathbf{U}_n\cdot\mathbf{S}_n\cdot\mathbf{V}_n{}^T \quad (2)$$

Assuming all the reactions were first-order reactions, $\mathbf{V}_n{}^T$ was fit as follows by least-squares fitting with a sum of single-exponential functions.

$$\mathbf{V}_n{}^T = \mathbf{C}\cdot[\exp(-t_i/\tau_1), \exp(-t_i/\tau_2), ..., \exp(-t_i/\tau_k), 1]^T$$
$$\text{where} \quad \tau_1 < \tau_2 < ... < \tau_k \quad (3)$$

Matrix **C** contained coefficient values of exponential function vectors $\exp(-t_i/\tau_j)$, where t_i represents the acquisition time corresponding to that of matrix **A**. The minimal number needed to adequately fit $\mathbf{V}_n{}^T$ was chosen as the number of exponential functions k. In this study, k equaled 1 and 2, which correspond to the formation of the meta-I/meta-II mixture from meta-I only and the formation and decay of the mixture, respectively. On the basis of eqs 1−3, data matrix **A** can be expressed as follows:

$$\mathbf{A} \approx \mathbf{U}_n\cdot\mathbf{S}_n\cdot\mathbf{C}\cdot$$
$$[\exp(-t_i/\tau_1), \exp(-t_i/\tau_2), ..., \exp(-t_i/\tau_k), 1]^T \quad (4)$$

The jth column of the product of matrices $\mathbf{U}_n$, $\mathbf{S}_n$, and **C** is the b-spectrum that denotes the spectral change in a single-exponential decay with time constant τ_j. The $(k + 1)$th column of the matrix is the b_0 spectrum, which corresponds to the bleached state. Figures 1−4 are shown with oppositely signed b-spectra for easy comparison.

RESULTS

Figure 1 shows absorption spectra of chloride- and nitrate-bound forms of mfas green, and spectral changes observed on the millisecond time scale after irradiation of these pigments with an orange light pulse. Absorption maxima of chloride- and nitrate-bound forms were 534 and 505 nm, respectively (Figure

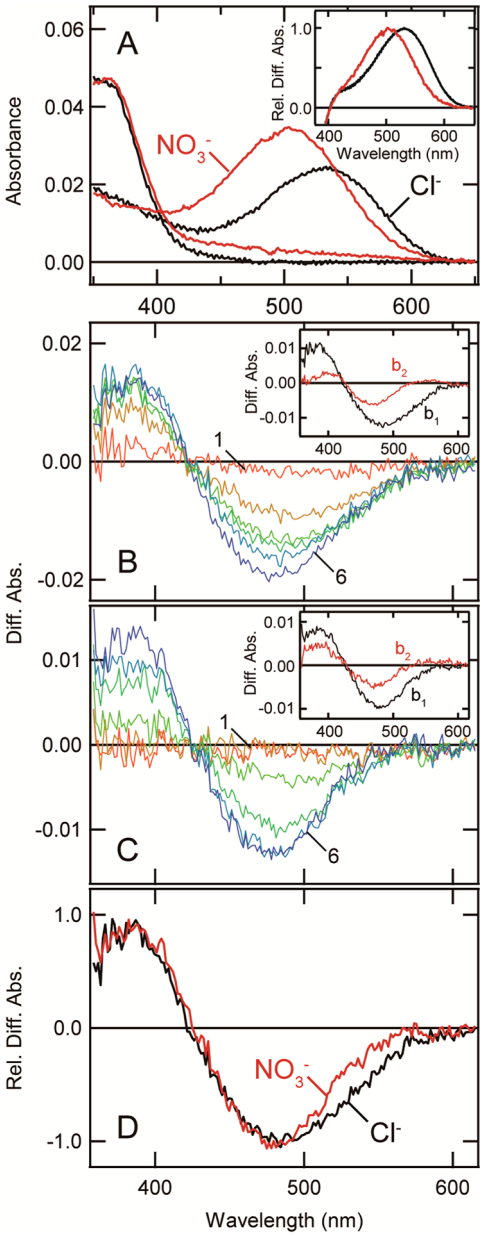

Figure 1. Effect of chloride on the absorption spectrum and reaction processes of mfas green. (A) Absorption spectra of chloride-bound (black) and nitrate-bound (red) mfas green before and after irradiation with >500 nm light for 5 min at 4 °C in the presence of 5 mM hydroxylamine (pH 7.0). These spectra were recorded using a Shimadzu UV-2400 spectrophotometer. The inset shows difference spectra of chloride-bound (black) and nitrate-bound (red) mfas green, where difference absorbances at the maxima were normalized. (B and C) Series of difference spectra of chloride-bound (B) and nitrate-bound (C) mfas green after irradiation with >520 nm light at 4 °C. These spectra were calculated by subtracting the spectra at 9.7 ms from those taken 19.4, 29.1, 67.9, 155, 446, and 892 ms after the irradiation (curves 1−6, respectively). The spectra were measured with the CCD spectrophotometer. The insets show b-spectra that are calculated by SVD analysis of the spectral data shown in the main panel, followed by global fitting. Details are described in the text. (D) b_1 spectra of chloride-bound (black) and nitrate-bound (red) mfas green, where absorbances at the negative difference maxima are normalized. They are identical to the b_1 spectra shown in the insets of panels B and C except for the vertical scale.

1A). The difference in absorption maximum between chloride- and nitrate-bound forms (29 nm) is typical for green pigments such as human green (25 nm)[11] and gecko green (31 nm)[8] and is smaller than those observed in red pigments such as chicken and human reds (45 and 35 nm, respectively).[10,11]

As previously shown,[7] irradiation of these pigments caused the formation of meta-I and subsequent decays into mixtures of meta-I and meta-II on the millisecond time scale. The spectral changes during these conversions are shown in panels B and C of Figure 1, as the difference spectra calculated by subtracting the spectra measured 9.7 ms after the irradiation from the spectra measured at selected times after the irradiation. These spectral changes and those monitored at later times were then analyzed by SVD and global fitting procedures, and two b-spectra (b_1 and b_2) were calculated (insets of panels B and C of Figure 1). Under our experimental conditions,[7] the b_1 spectrum represents the conversion from meta-I to a mixture of meta-I and meta-II, and it can therefore be regarded as the difference spectrum between meta-I and meta-II. The b_2 spectrum contains the spectral components of the reverse reaction to the original pigments from the mixture of meta-I and meta-II, and the decomposition reaction of the mixture of meta-I and meta-II to retinal and opsin. The time constants corresponding to the b_1 and b_2 spectra were 108 ms (τ_1) and 115 s (τ_2) for the chloride-bound form and 2.01 s (τ_1) and 187 s (τ_2) for the nitrate-bound form, which were in good agreement with those previously obtained.[7] Figure 1D shows the superimposed spectra after normalization of the respective b_1 spectra obtained from chloride- and nitrate-bound forms. Although these spectra are similar to each other, the spectrum of meta-I in the chloride-bound form is somewhat broader than that in the nitrate-bound form. The absorption maximum of meta-I in the chloride-bound form is ∼5 nm longer than that in the nitrate-bound form. The fact that meta-I of the chloride-bound form exhibits a spectral shape and maximum different from those of the nitrate-bound form indicates that the chloride is still bound to the protein moiety of meta-I and perturbs its spectrum.

We next tested the effect of different amino acids at the primary chloride-binding site at position 197. Of the 19 possible single-site mutants, 13 were successfully expressed and formed pigments by binding 11-*cis*-retinal. These mutants were also prepared in the presence of chloride or nitrate and subjected to similar spectroscopic analyses (Figures 2−4 and Table 1). Eleven of the 13 mutants exhibited varying red shifts of absorption maxima upon chloride binding. The original histidine exhibited the most red-shifted λ_{max} of all the expressed pigments. Close inspection of the data revealed that the H197 mutants could be categorized into the following three groups.

The first group (group 1 in Table 1) contains mutants that exhibit a chloride effect similar to that of WT. This group contains M, N, K, Q, A, and L mutants. As shown in Figure 2, these mutants had an absorption maximum at ∼500 nm in the presence of nitrate (Figure 2B), but the absorption maximum shifted to a longer wavelength in the presence of chloride (Figure 2A). The extents of the shifts of absorption maxima were, however, not as prominent compared to that of the WT. Interestingly, the absorption maximum of meta-I of each mutant showed no anion dependency (Figure 2C−H), although its absorption maximum ranged between 478 and 485 nm. Additionally, the relative rate constants of the conversion from meta-I to meta-II were as small as that of WT in the presence of nitrate (Figure 2J) and became larger in the presence of chloride like that of the WT (Figure 2I). There

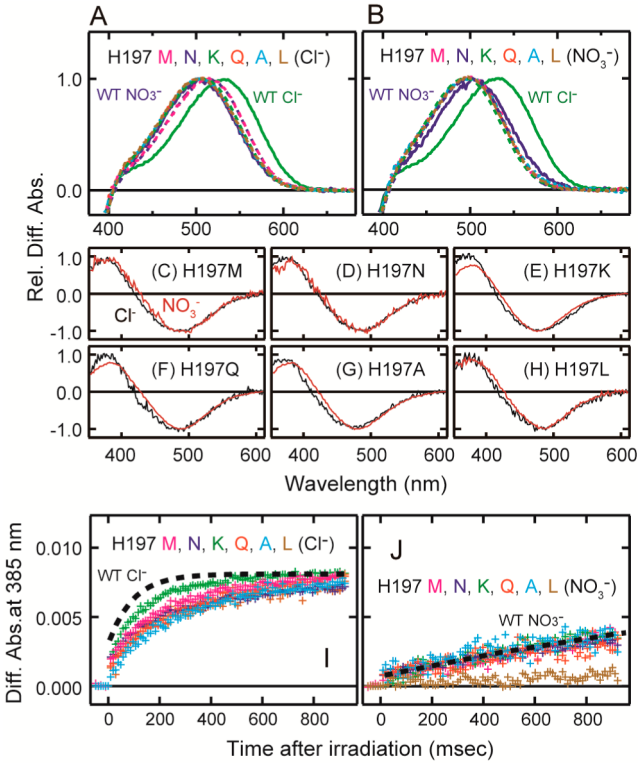

Figure 2. Effect of chloride on the absorption spectra of the dark state and meta-I and formation of meta-II in group 1 mutants. (A and B) Difference spectra of the chloride-bound (A) and nitrate-bound (B) mutants before and after irradiation with >500 nm light at 4 °C in the presence of 5 mM hydroxylamine (pH 7.0). The spectra of the mutants are colored magenta (H197M), blue (H197N), green (H197K), orange (H197Q), light blue (H197A), and ocher (H197L). (C–H) b_1 spectra of chloride-bound (black) and nitrate-bound (red) mutants, where absorbances at the negative difference maxima are normalized. Spectral measurements were taken at 4 °C: (C) H197M, (D) H197N, (E) H197K, (F) H197Q, (G) H197A, and (H) H197L. (I and J) Formation kinetics of meta-II in chloride-bound (I) and nitrate-bound (J) forms of mutants at 4 °C. Kinetics of the respective mutants are colored magenta (H197M), blue (H197N), green (H197K), orange (H197Q), light blue (H197A), and ocher (H197L). Kinetics of WT are shown as a dashed line.

was no correlation between the shifts in absorption maxima and changes in rate constants.

The second group (group 2 in Table 1) contains D and G mutants, which showed no chloride effect (Figure 3). That is, absorption maxima of these mutants and their meta-I forms showed no difference between chloride and nitrate preparations (Figure 3A–D). The relative rate constants from meta-I to meta-II also showed no change (Figure 3E,F). These mutants, therefore, seem not to bind chloride or nitrate.

The third group (group 3 in Table 1) contains Y, T, F, V, and I mutants (Figure 4). These mutants showed wavelength shifts of absorption maxima upon chloride binding similar to those of group 1 mutants, although the shifts were not as prominent as that of WT (Figure 4A). The salient feature of these mutants is the elevated rate constant of meta-I decay. These mutants exhibited relative rate constants of meta-I decay 5–35 times faster than that of WT in the nitrate-bound form (Figure 4I and Table 1). Remarkably, some of the mutants in this group showed an increase in the relative rate constant over

Table 1. Spectroscopic Characterization of WT and His197 Mutants of mfas Green

		λ_{max} (nm) of mfas green		λ_{max} (nm) of MI		relative rate constant[a]	
group	sample	Cl^-	NO_3^-	Cl^-	NO_3^-	Cl^-	NO_3^-
1	WT	534	505	484	479	100	6
	H197M	516	500	485	485	30	4
	H197N	515	500	485	485	30	5
	H197K	508	497	479	478	84	5
	H197Q	507	500	484	485	51	2
	H197A	506	500	479	479	36	4
	H197L	505	500	484	485	26	3
2	H197D	489	489	484	482	10	11
	H197G	489	489	479	479	7	7
3	H197Y	511	497	464	464	273	202
	H197T	510	500	479	478	82	50
	H197F	506	497	484	478	72	33
	H197V	503	502	464	464	204	104
	H197I	503	502	464	464	209	56

[a]The relative rate constant of meta-I in each mutant is shown relative to that in the chloride-bound WT form.

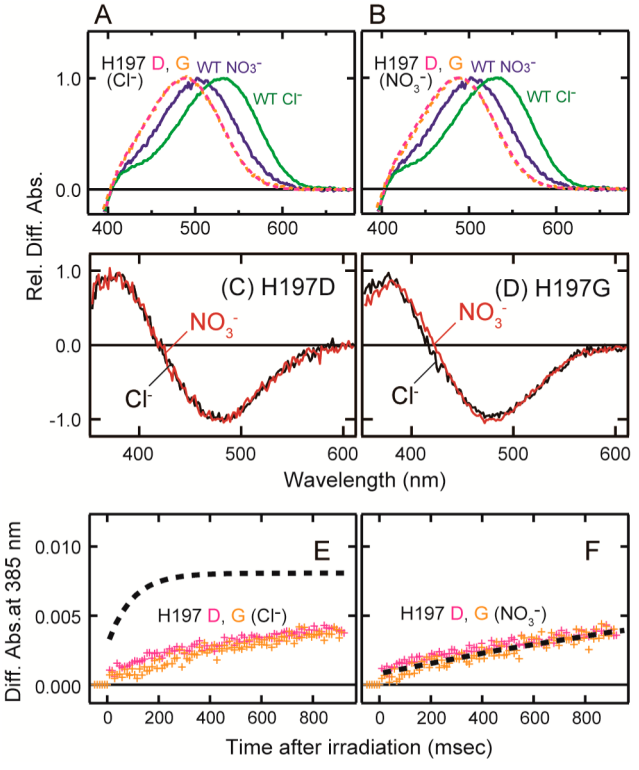

Figure 3. Effect of chloride on the absorption spectra of the dark state and meta-I and formation of meta-II in group 2 mutants. (A and B) Difference spectra of the mutants in the presence of chloride (A) and nitrate (B) before and after irradiation with >500 nm light at 4 °C in the presence of 5 mM hydroxylamine (pH 7.0). The spectra of the mutants are colored magenta (H197D) and yellow (H197G). (C and D) First b-spectra of mutants in the presence of chloride (C) and nitrate (D), where absorbances at the negative difference maxima are normalized: (C) H197D and (D) H197G. (E and F) Kinetics of formation of meta-II mutants in the presence of chloride (E) and nitrate (F). Kinetics of the respective mutants are colored magenta (H197D) and yellow (H197G). Kinetics of WT are shown as a dashed line.

dx.doi.org/10.1021/bi300995s | *Biochemistry* 2012, 51, 10017–10023

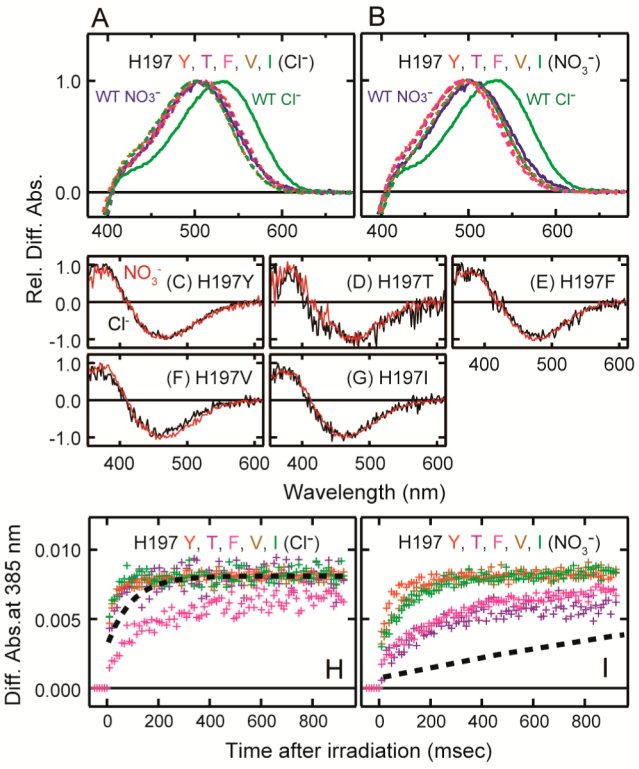

Figure 4. Effect of chloride on the absorption spectra of the dark state and meta-I and formation of meta-II in group 3 mutants. (A and B) Difference spectra of the chloride-bound (A) and nitrate-bound (B) mutants before and after irradiation with >500 nm light at 4 °C in the presence of 5 mM hydroxylamine (pH 7.0). The spectra of the mutants are colored orange (H197Y), purple (H197T), magenta (H197F), ocher (H197V), and green (H197I). (C to G) First b-spectra of chloride-bound (black) and nitrate-bound (red) mutants, where absorbances at the negative difference maxima are normalized: (C) H197Y, (D) H197T, (E) H197F, (F) H197V, and (G) H197I. (H and I) Kinetics of formation of meta-II in chloride-bound (H) and nitrate-bound (I) forms of mutants. Kinetics of the mutants are colored orange (H197Y), purple (H197T), magenta (H197F), ocher (H197V), and green (H197I). Kinetics of WT are shown as a dashed line.

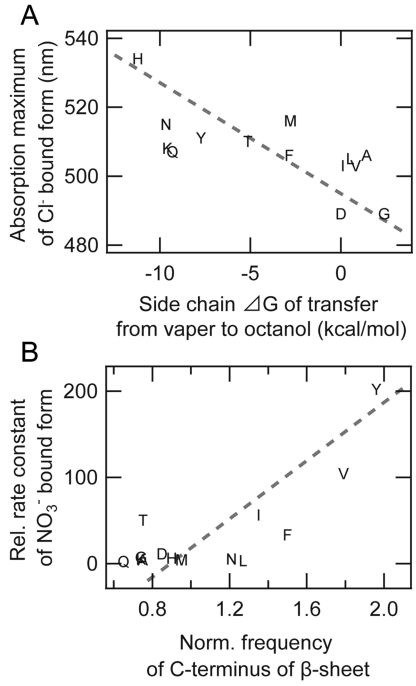

Figure 5. Relationship between spectral and thermal properties of mfas green and physicochemical properties of the amino acid at position 197. (A) Absorption maximum of the chloride-bound form of each mutant plotted as a function of ΔG of transfer from vapor to octanol. Characters in the figure show the points of the mutants. The dashed line drawn through the points is a linear regression of data. A correlation coefficient is given in the text. (B) Rate constant of decay of meta-I of the nitrate-bound form of each mutant plotted as a function of the normalized frequency of the C-terminus of the β-sheet of the residue at position 197. Characters in the figure show the points of the mutants. The dashed line drawn through the points is a linear regression of data. A correlation coefficient is given in the text.

that of the WT in the chloride-bound form (Figure 4H and Table 1).

DISCUSSION

We have investigated the role of H197 in the effect of chloride on the L group pigment by characterizing a set of site-directed mutants. Spectroscopic analyses of mutants showed that mutants exhibited varying chloride effects, and therefore, the histidine residue at position 197 is not essential for the chloride effect. However, the mutants can be categorized into three groups according to the type of chloride effect. Hereafter, we discuss the effect of different amino acids at the primary chloride-binding site.

Effect of Chloride on the Absorption Maximum of the Dark State. Because 11 mutants exhibited chloride-dependent red shifts of the absorption maxima, we searched for a total of 544 descriptors of the physicochemical properties of natural amino acids registered in AAindex[21] to understand the relationship between the extent of the red shift and the physicochemical properties of amino acids. We found that the polarities of amino acids (ΔG of transfer from vapor to octanol) correlated well with the red shift of absorption maxima [correlation coefficient of 0.71; $p < 0.005$ (Figure 5A)].[22] It should be noted that a weak but significant correlation (correlation coefficient of 0.56) is seen even when the values of H, D, and G are omitted. Thus, it is likely that chloride forms a dipole with the residue at position 197 and interacts with the chromophore. This is consistent with our previous results from the UV−vis and FTIR spectroscopies of chloride-bound, chloride-depleted (anion-free), and nitrate-bound iodopsins (chicken red).[23] Namely, we found that the chromophore bands in the FTIR difference spectra were almost identical among the three iodopsin forms, except for the C═C ethylenic vibrational band near 1500 cm^{-1}, and concluded that chloride acts as a dipole after forming a dipole with the nearby histidine. It should be noted that these experiments using mfas green clearly showed that the H197Y mutant exhibited a red-shifted absorption maximum upon chloride binding. However, mouse green that has a tyrosine at this position does not show the red shift (both mfas green and mouse green have K200).[24] These results suggest that there is another amino acid residue(s) involved in chloride binding that would account for the differences between mfas green and mouse green.[24,25]

In contrast to the chloride-bound forms, nitrate-bound forms show modest shifts of absorption maxima, indicating that nitrate binding does not severely affect the electronic state of the chromophore. This is interesting because we have already

dx.doi.org/10.1021/bi300995s | Biochemistry 2012, 51, 10017−10023

demonstrated that nitrate and chloride compete for the same binding site in iodopsin, by measuring the apparent dissociation constant of chloride as a function of nitrate concentration in the iodopsin sample.[26] In addition, we demonstrated that nitrate-bound iodopsin showed an FTIR spectrum identical with that of anion-free iodopsin, suggesting that nitrate binding does not perturb the chromophore.[23] If the results obtained from iodopsin can be applied to mfas green, the simplest explanation is that the site to which nitrate binds is far from the chromophore, and the anion-binding site would move toward the chromophore upon chloride binding.[23]

Effect of Chloride on the Absorption Maximum of Meta-I. Absorption maxima of the resting state of mutants in the chloride-bound forms differ by 45 nm, ranging from 489 to 534 nm, while those of meta-I differ by 20 nm, ranging from 464 to 484 nm. This indicates that the environment of the chromophore changes during meta-I formation. More importantly, most mutants exhibited absorption maxima of meta-I that are insensitive to the replacement of the anion. The exceptions were WT and H197F, but even in these pigments, the difference between chloride- and nitrate-bound forms was only 5 nm. These results, therefore, suggest that the chromophore of meta-I is more distant from the anion-binding site than that of the resting state.

Effect of Chloride on Meta-I Decay. Decay of meta-I of chloride-bound mfas green was ∼20 times faster than that of the nitrate-bound form, indicating that rapid decay of meta-I is one of the effects of chloride binding. However, when histidine at position 197 was replaced with the residues in group 3, meta-I decay changed dramatically. That is, decay of meta-I in the nitrate-bound preparation became 5−30 times faster than that of WT and approached that in the chloride-bound preparation. Additionally, three of the six group 3 mutants exhibited decay of meta-I that was faster than that of WT in the chloride-bound preparations. These mutants still have a chloride-binding site and bind to chloride, as group 3 mutants showed red shifts of absorption maxima when nitrate was replaced with chloride. We found that among 544 descriptors of the physicochemical properties of natural amino acids registered in AAindex,[21] the rate of meta-I decay correlated well with the frequencies of amino acids that appear in β-sheets [correlation coefficient of 0.79; $p < 0.005$ (Figure 5B)].[12] From the $\Delta\Delta G$ measurements of amino acids, a strong correlation was suggested between amino acids frequently present in β-sheets and β-sheet stability,[27] although some ambiguity still remained.[28] According to the three-dimensional structure of rhodopsin, H197 is situated at the C-terminal site of sheet β-4, which forms an antiparallel β-sheet with sheet β-3.[29] Therefore, the presence of amino acid residues predisposed to form a β-sheet at this position could accelerate the conversion from meta-I to meta-II. However, comparison of the three-dimensional structure of metarhodopsin II with that of rhodopsin shows that the β-sheet structure does not deviate greatly from the structure of rhodopsin.[30] Additionally, there are some indications that metarhodopsin I has a structure very similar to that of rhodopsin.[31] Furthermore, mutational analysis of the amino acid at position 181 (corresponding to position 197 in mfas green) of bovine rhodopsin did not show a significant effect on the absorption maximum.[32] Thus, the amino acid residue at position 197 (181) would be in different environments between rhodopsin and the L group pigment. Structural knowledge of the L group pigment is therefore required to improve our understanding of the chloride effect.

CONCLUSION

The amino acid residue at position 197 acts as the Schiff base counterion in invertebrate visual pigments and was replaced with histidine after the acquisition of a new counterion at position 113 during the course of molecular evolution of L group cone visual pigments.[33] The histidine at this position serves as a part of the chloride-binding site and red shifts the absorption maximum of visual pigments.[11] In addition, recent experiments showed that chloride binding accelerates meta-I decay and increases the amount of the active state in the mixture of the active state and its precursor.[7] The study presented here indicates that the polarity of the amino acid situated at this position is important for the red shift of the absorption maximum, and histidine produces the most red-shifted absorption maximum. Additionally, the substitutions at position 197 with residues with a strong propensity to form β-sheet accelerate the formation of the active state as much as that of the WT in the chloride-bound form. Although it is difficult to reach conclusions from the finding of only one residue that has a strong propensity to form β-sheet, the results suggest some relationship between chloride binding and β-sheet formation that accelerates conversion to the active state. Therefore, the acquisition of histidine at the chloride-binding site resulting in rapid formation of the active state may have been an essential step for the emergence of vertebrate red-sensitive cone visual pigments.

AUTHOR INFORMATION

Corresponding Author

*Telephone: +81-75-753-4213. Fax: +81-75-753-4210. E-mail: shichida@rh.biophys.kyoto-u.ac.jp.

Present Address

[†]Department of Biochemistry, University of Toronto, Toronto, Ontario M5S 1A8, Canada.

Funding

This work was supported in part by Grants-in-Aid for Scientific Research from the Japanese Ministry of Education, Culture, Sports, Science and Technology to Y.S.

Notes

The authors declare no competing financial interest.

ACKNOWLEDGMENTS

We thank Dr. S. Koike for providing us with 293T cell lines and Prof. R. S. Molday for the generous gift of a Rho1D4-producing hybridoma. We also thank Drs. H. Imai and A. Onishi for technical advice about protein expression and spectroscopy during the early stage of the experiments. We are also grateful to Dr. T. Matsuyama for critical reading of the manuscript and invaluable comments.

ABBREVIATIONS

λ_{max}, absorption maximum; CCD, charge-coupled device; FTIR, Fourier transform infrared; HEPES, *N*-(2-hydroxyethyl)-piperazine-*N*′-2-ethanesulfonic acid; CHAPS, 3-[(3-cholamidopropyl)dimethylammonio]-1-propanesulfonate; PC, L-α-phosphatidylcholine from egg yolk; CHAPS/PC, buffer solution that contains a mixture of CHAPS and PC; mfas, *M. fascicularis*; WT, wild type.

REFERENCES

(1) Hofmann, K. P., Scheerer, P., Hildebrand, P. W., Choe, H. W., Park, J. H., Heck, M., and Ernst, O. P. (2009) A G protein-coupled

receptor at work: The rhodopsin model. *Trends Biochem. Sci. 34*, 540–552.
(2) Shichida, Y., and Imai, H. (1998) Visual pigment: G-protein-coupled receptor for light signals. *Cell. Mol. Life Sci. 54*, 1299–1315.
(3) Yokoyama, S. (2008) Evolution of dim-light and color vision pigments. *Annu. Rev. Genomics Hum. Genet. 9*, 259–282.
(4) Okano, T., Kojima, D., Fukada, Y., Shichida, Y., and Yoshizawa, T. (1992) Primary structures of chicken cone visual pigments: Vertebrate rhodopsins have evolved out of cone visual pigments. *Proc. Natl. Acad. Sci. U.S.A. 89*, 5932–5936.
(5) Imai, H., Kuwayama, S., Onishi, A., Morizumi, T., Chisaka, O., and Shichida, Y. (2005) Molecular properties of rod and cone visual pigments from purified chicken cone pigments to mouse rhodopsin in situ. *Photochem. Photobiol. Sci. 4*, 667–674.
(6) Shichida, Y., and Matsuyama, T. (2009) Evolution of opsins and phototransduction. *Philos. Trans. R. Soc. London, Ser. B 364*, 2881–2895.
(7) Sato, K., Yamashita, T., Imamoto, Y., and Shichida, Y. (2012) Comparative studies on the late bleaching processes of four kinds of cone visual pigments and rod visual pigment. *Biochemistry 51*, 4300–4308.
(8) Crescitelli, F. (1977) Ionochromic behavior of Grecko visual pigments. *Science 195*, 187–188.
(9) Fager, L. Y., and Fager, R. S. (1979) Halide control of color of the chicken cone pigment iodopsin. *Exp. Eye Res. 29*, 401–408.
(10) Shichida, Y., Kato, T., Sasayama, S., Fukada, Y., and Yoshizawa, T. (1990) Effects of chloride on chicken iodopsin and the chromophore transfer reactions from iodopsin to scotopsin and B-photopsin. *Biochemistry 29*, 5843–5848.
(11) Wang, Z., Asenjo, A. B., and Oprian, D. D. (1993) Identification of the Cl^--binding site in the human red and green color vision pigments. *Biochemistry 32*, 2125–2130.
(12) Chou, P. Y., and Fasman, G. D. (1978) Prediction of the secondary structure of proteins from their amino acid sequence. *Adv. Enzymol. Relat. Areas Mol. Biol. 47*, 45–148.
(13) Nathans, J. (1990) Determinants of visual pigment absorbance: Identification of the retinylidene Schiff's base counterion in bovine rhodopsin. *Biochemistry 29*, 9746–9752.
(14) Onishi, A., Koike, S., Ida, M., Imai, H., Shichida, Y., Takenaka, O., Hanazawa, A., Komatsu, H., Mikami, A., Goto, S., Suryobroto, B., Kitahara, K., and Yamamori, T. (1999) Dichromatism in macaque monkeys. *Nature 402*, 139–140.
(15) Oprian, D. D., Asenjo, A. B., Lee, N., and Pelletier, S. L. (1991) Design, chemical synthesis, and expression of genes for the three human color vision pigments. *Biochemistry 30*, 11367–11372.
(16) Imai, H., Kojima, D., Oura, T., Tachibanaki, S., Terakita, A., and Shichida, Y. (1997) Single amino acid residue as a functional determinant of rod and cone visual pigments. *Proc. Natl. Acad. Sci. U.S.A. 94*, 2322–2326.
(17) Kayada, S., Hisatomi, O., and Tokunaga, F. (1995) Cloning and expression of frog rhodopsin cDNA. *Comp. Biochem. Physiol., Part B: Biochem. Mol. Biol 110*, 599–604.
(18) Nagata, T., Terakita, A., Kandori, H., Kojima, D., Shichida, Y., and Maeda, A. (1997) Water and peptide backbone structure in the active center of bovine rhodopsin. *Biochemistry 36*, 6164–6170.
(19) Morizumi, T., Imai, H., and Shichida, Y. (2005) Direct observation of the complex formation of GDP-bound transducin with the rhodopsin intermediate having a visible absorption maximum in rod outer segment membranes. *Biochemistry 44*, 9936–9943.
(20) Hug, S. J., Lewis, J. W., Einterz, C. M., Thorgeirsson, T. E., and Kliger, D. S. (1990) Nanosecond photolysis of rhodopsin: Evidence for a new, blue-shifted intermediate. *Biochemistry 29*, 1475–1485.
(21) Nakai, K., Kidera, A., and Kanehisa, M. (1988) Cluster analysis of amino acid indices for prediction of protein structure and function. *Protein Eng. 2*, 93–100.
(22) Radzicka, A., and Wolfenden, R. (1988) Comparing the Polarities of the Amino Acids: Side-Chain Distribution Coefficients between the Vapor Phase, Cyclohexane, 1-Octanol, and Neutral Aqueous Solution. *Biochemistry 27*, 1664–1670.
(23) Hirano, T., Imai, H., and Shichida, Y. (2003) Effect of anion binding on the thermal reverse reaction of bathoiodopsin: Anion stabilizes two forms of iodopsin. *Biochemistry 42*, 12700–12707.
(24) Sun, H., Macke, J. P., and Nathans, J. (1997) Mechanisms of spectral tuning in the mouse green cone pigment. *Proc. Natl. Acad. Sci. U.S.A. 94*, 8860–8865.
(25) Davies, W. I., Wilkie, S. E., Cowing, J. A., Hankins, M. W., and Hunt, D. M. (2012) Anion sensitivity and spectral tuning of middle- and long-wavelength-sensitive (MWS/LWS) visual pigments. *Cell. Mol. Life Sci. 69*, 2455–2464.
(26) Tachibanaki, S., Imamoto, Y., Imai, H., and Shichida, Y. (1995) Effect of chloride on the thermal reverse reaction of intermediates of iodopsin. *Biochemistry 34*, 13170–13175.
(27) Minor, D. L., Jr., and Kim, P. S. (1994) Measurement of the β-sheet-forming propensities of amino acids. *Nature 367*, 660–663.
(28) Minor, D. L., Jr., and Kim, P. S. (1994) Context is a major determinant of β-sheet propensity. *Nature 371*, 264–267.
(29) Okada, T. (2004) X-ray crystallographic studies for ligand-protein interaction changes in rhodopsin. *Biochem. Soc. Trans. 32*, 738–741.
(30) Choe, H. W., Kim, Y. J., Park, J. H., Morizumi, T., Pai, E. F., Krauss, N., Hofmann, K. P., Scheerer, P., and Ernst, O. P. (2011) Crystal structure of metarhodopsin II. *Nature 471*, 651–655.
(31) Ruprecht, J. J., Mielke, T., Vogel, R., Villa, C., and Schertler, G. F. (2004) Electron crystallography reveals the structure of metarhodopsin I. *EMBO J. 23*, 3609–3620.
(32) Yan, E. C. Y., Kazmi, M. A., De, S., Chang, B. S. W., Seibert, C., Marin, E. P., Mathies, R. A., and Sakmar, T. P. (2002) Function of Extracellular Loop 2 in Rhodopsin: Glutamic Acid 181 Modulates Stability and Absorption Wavelength of Metarhodopsin II. *Biochemistry 41*, 3620–3627.
(33) Terakita, A., Koyanagi, M., Tsukamoto, H., Yamashita, T., Miyata, T., and Shichida, Y. (2004) Counterion displacement in the molecular evolution of the rhodopsin family. *Nat. Struct. Mol. Biol. 11*, 284–289.